

2006

S-Band Plasma Limiters for Electromagnetic Pulse Protection

Matthew Andersen

Follow this and additional works at: https://knowledge.e.southern.edu/senior_research



Part of the [Physics Commons](#)

Recommended Citation

Andersen, Matthew, "S-Band Plasma Limiters for Electromagnetic Pulse Protection" (2006). *Senior Research Projects*. 29.
https://knowledge.e.southern.edu/senior_research/29

This Article is brought to you for free and open access by the Southern Scholars at KnowledgeExchange@Southern. It has been accepted for inclusion in Senior Research Projects by an authorized administrator of KnowledgeExchange@Southern. For more information, please contact jspears@southern.edu.

S-Band Plasma Limiters for Electromagnetic Pulse Protection

Matthew Andersen

Southern Adventist University
Southern Scholars
&
Physics Research Report
Final Draft

In conjunction with:
Accurate Automation Corporation

2006

Table of Contents

Table of Contents	2
Schedule of Performed Work.....	3
Introduction.....	4
Technical Background.....	5
Purpose	8
Testing.....	9
Initial S-band Testing	9
Development of UWB Source.....	14
Development of TE ₂₀ Limiting.....	17
Conclusions.....	24
References.....	25

Schedule of Performed Work

Week of:	Hours	Work Performed
August 22	8	Developed a high power, Ultra Wide Band source with fast rise time and high power using existing equipment. Tried various gas mixtures in waveguide.
September 5	11	Collected data with runs using UWB source. Did some analysis on this data. Began retesting of normal S-band high power microwaves (HPM).
September 12	2	Took additional data using HPM source.
September 19	6	Additional testing: found one of our crossguides is bad among other problems. Re-achieved high power output.
October 3	2	Designed new test section for the detection of modes other than TE ₁₀ .
October 17	3	Looked for and ordered several new parts: two directional couplers, a terminator, and straight section.
October 24	4	Designed TE ₂₀ mode launcher using X-band magnetron, magic tee, and block of aluminum.
October 31	3	Designed radiation enclosure for S-band HPM launcher.
November 7	4	Cut up ordered straight section to create a multimode detector.
November 14	4	Assembled magic tee and machined aluminum into multimode launcher.
January 9	8	Fixed magnetron and began testing TE ₂₀ mode launcher.
January 30	6	Build multimode measuring section. Testing of TE ₂₀ mode, had some problems with attenuation.
February 6	5	Figured out attenuation problems in diodes and test section. Ordered some smaller N-type attenuators.
February 13	7	Took data using 1, 2, and 3 needle setups.
February 20	8	Made adjustments to multiple needle setup, optimizations, etc and took some more data. Analyzed data.
March 13	12	Re-setup the UWB experiment for use with the new enclosure, cabling, and multiple needle test section. Took data. Some problems occurred.
March 20	6	Switched back to single needle configuration for additional testing with the UWB source.

Currently, we have finished the project and the requirements for the given contract. We have applied for some additional time and money to continue testing and development within the failure modes. If signed the option/addition to the current contract with begin in May.

The time listed in the above table totals 99 hours and only includes laboratory and part design / fabrication time. It does not include research or report writing time.

Introduction

According to the September 2001 *Popular Mechanics*, the United States and all its electronic equipment currently face as serious threat from electromagnetic waves via High Powered Microwaves (HPM) and Ultra Wide Band (UWB) radio frequency (RF) sources. This electronic equipment, whether consumer, business, or government, is susceptible to power surges from sources ranging from lightning strikes to electromagnetic pulse (EMP) bombs. *Popular Mechanics* says that “[a]ny nation with even a 1940s technology base could make [EMP bombs]. The threat of E-bomb proliferation is very real” [1]. In response to an attack such as described, research into protection devices is needed. Plasma limiters are the result of such research. They can provide highly reliable, front-end protection from these surges in a low-cost, easily implemented manner.

Simply described, plasma limiters are fuses or surge protectors that protect sensitive electronics from disruption or destruction by high power RF. Limiters are normally passive and do not affect the operation of the circuitry. However, when a high power RF pulse is incident, the limiter is activated. As long as the threat energy is present, the transmitted power is ‘limited’ to zero (or near zero) and the damaging energy of the incident power is reflected. Once the RF pulse ceases, the plasma limiter recovers and returns to its normally passive state.

Currently, two types of transient suppression devices capable of providing high RF power protection exist. The first includes solid state devices such as metal oxide varistors (MOV) and silicon avalanche diodes. These devices have fast activation times, but are limited in the incident power they can withstand. Conventional gas-discharge tubes comprise the second. These tubes are essentially spark gaps in which an arc discharge occurs when a RF pulse is applied. They can withstand more power than the solid state devices but have a slower activation time.

Conventional gas discharge devices are the most widely utilized and have been used for decades on communications equipment to protect from long-pulse, disruptive electromagnetic interference (EMI) and electromagnetic pulse (EMP). These devices have inherently slow rise times, typically microseconds, and tend to be quite bulky; however, they can protect equipment from high amplitude electric fields and large currents [2].

Technical Background

The concept of a plasma limiter as protection against high power EMI and microwaves is a simple one. For example, a plasma limiter in a waveguide transmission line receiving a fixed frequency microwave signal is shown in Figure 1. During normal operation, microwaves propagate through the waveguide, shown in Figure 1(a). The plasma limiter contains an electrode with a very fine point mounted to one of the parallel plates. Figure 1(b) shows incident HPM propagating through a waveguide. Once the HPM reaches the plasma limiter, a discharge occurs (ideally, instantaneously) and all the incident microwave radiation is reflected, shown in Figure 1(c).

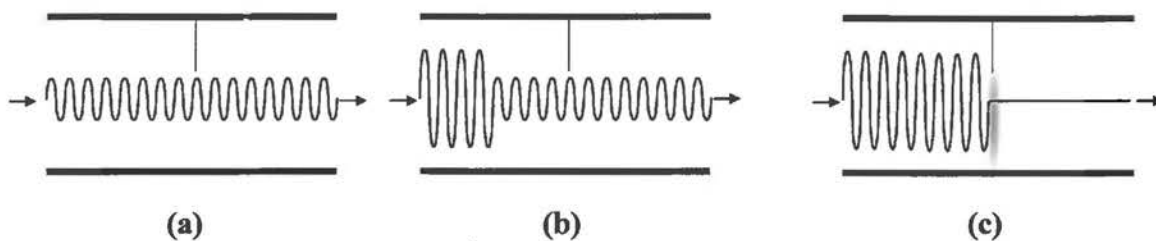


Figure 1: Schematic demonstrating the plasma limiter concept (a) during normal operation, (b) just before incident HPM reaches the limiter, and (c) after the limiter has discharged

This process protects downstream equipment from the potentially damaging microwave radiation. For breakdown to initiate, free electrons must exist within the cell gap. UV radiation, radioactive decay, or cosmic rays can create these electrons via electron emission. The first two require some active pre-ionization and the latter occurs naturally but with significant statistical time delays [3].

Another mechanism by which electrons may be introduced into the cell gap is field emission [4]. The high electric field at the cathode is a result of the applied electric field and the fine point geometry of the cathode. When the electric field at the cathode is extremely high it will pull the electrons away, transforming the potential well into a potential barrier of finite width. As a result, the electrons escape the metal cathode by tunneling. There is no significant statistical delay with this process and no active devices needed to introduce electrons into the cell gap.

Once the electrons are introduced into the gap, a streamer discharge begins. To understand streamer discharge, the mechanisms of electrical breakdown must be examined [5]. When attempting to describe electrical breakdown, the Townsend breakdown mechanism is often used [6]. Townsend breakdown initially starts with a free electron located somewhere between a pair of electrodes. The free electron experiences a force that accelerates the electron until it collides with a neutral atom or molecule. If the electron has gained enough kinetic energy, the collision is inelastic and the neutral atom is ionized. The collision results in two free electrons and one positive ion. The process repeats and the two electrons become four, and so on. This process is known as an electron avalanche. If enough avalanches occur over a period of time, the gas temperature increases thereby lowering the channel resistance. The gap resistance then drops to a point where the electrical driving circuit heats the channel more efficiently. The gap resistance continues to drop rapidly along with the gap voltage to very low values at which time complete electrical breakdown (Townsend breakdown) is said to have occurred.

Many, but not all, of the processes observed in gaseous breakdown can be explained using the Townsend mechanism. It falls short in explaining breakdown in overvoltage gaps (gaps in which the applied voltage is $>20\%$ of the DC breakdown voltage). Mainly, the Townsend mechanism does not explain the short formative times (time from when the voltage is applied to when complete electrical breakdown occurs) observed experimentally. There are two events involved in the overvoltage gaps that the Townsend mechanism does not consider [7]. The first involves photoemission and photoionization. As the electron avalanches are forming and growing, some of the metastable states return to ground state and emit energetic photons. A metastable state occurs when an electron collides with an atom but does not transfer enough energy to ionize the atom. This causes an electron(s) to become excited into a higher state with the property that it is unable to immediately return to the ground state. Once some additional energy is received by the atom the electron(s) can increase its state again, return to ground, and emit energetic photons. These photons may be absorbed by other atoms in neutral and/or excited states, resulting in their ionization.

The other process not considered is the self-generated electric field of the space charge in the avalanche. As the avalanche increases in numbers of electrons, so does its self-generated electric field, increasing linearly. When the self-generated electric field becomes on the order of

the external electric field due to the gap voltage, significant changes in electron energies and ionization will occur locally.

Photoemission, photoionization, and the development of an intense electric field due to space charge are processes that dominate streamer discharge. A streamer discharge starts out much like a Townsend breakdown with an initial electron avalanche. At high electric fields and moderate pressures, the electron avalanche will grow such that the self-generated electric field at the head of the avalanche becomes roughly the size of the electric field across the gap. The self-generated electric field causes locally intense ionization at the head of the avalanche, and results in photoemission and photoionization that develop additional electron avalanches. A schematic of the temporal development of a streamer discharge is shown in Figure 2.

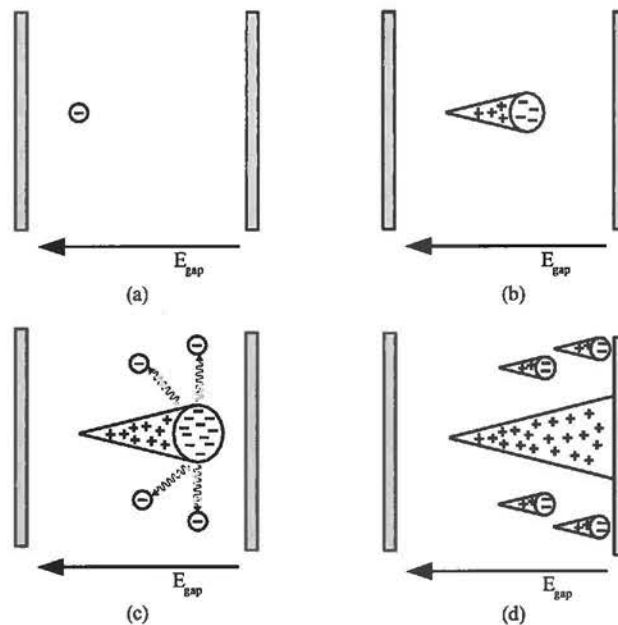


Figure 2: Streamer discharge development across a plane parallel gap (a) initial free electron, (b) initial electron avalanche, (c) intense electric field due to space charge starts photoionization, and (d) initial electron avalanche multiplies into multiple electron avalanches.

The temporal development of streamers is a very fast process. The speed at which these streamers can cross the cell gaps is dependent on the magnitude of the applied voltage, gas pressure, and the non-uniformity of the E-field. Streamer velocities can be as high as 4×10^6 m/sec or 1.3% the speed of light [8].

Once the streamer crosses the cell gap, a complex thermal process increases the channel conductivity. At this time, the discharge is fully developed and the gap is considered to be conducting. It has been shown experimentally that these three processes,

- electron field emission,
- streamer discharge, and
- increased channel conductivity

can occur very quickly when the electric fields across the gap and near the cathode are high enough [9].

When the applied voltage is removed, the gas within the cell gap requires a finite period of time to return to its pre-ionized state. This is the relaxation or deionization time of the particular ionized gas. Deionization is a complex process composed of many phenomena. Within the gas itself, deionization will occur predominately via diffusion, recombination, and attachment. For a plasma limiter, the relaxation time determines the recovery time of the overall system.

By utilizing and optimizing these processes plasma limiters offer several advantages over the present state of the art gas discharge protection devices:

- extremely fast turn-on times,
- simple geometry and integration into existing equipment, and
- no active pre-ionization equipment requirement [2].

Purpose

The goal of the first phase of this project was to prove the feasibility of a plasma limiter in an S-band waveguide configuration capable of 1) extremely fast response time, and 2) the ability to reflect high peak and average incident disruptive RF power. The challenge in developing such a device lies in the fact that these two performance characteristics are incompatible in conventional transient protective devices. For example, solid state devices such as silicon avalanche diodes have extremely fast turn-on times (<1 psec) and even high peak power capability (>100 kW) but have low average power handling capability (< 10 W). Conversely, conventional gas discharge tubes can easily handle average powers > 10 kW but have inherently slow turn-on times (> 100 nsec) [2].

The project's second phase goal was to develop a working proof-of-principle demonstration of an S-band plasma limiter which displays the best characteristics of both conventional devices: large power handling capability and fast response time. As part of the process, the following technical challenges were addressed:

- UWB source design and development,
- Mixed / multimode testing,
- Test section design and fabrication,
- Ultra fine needle positioning, and
- Easy integration into existing equipment.

Testing

Initial S-band Testing

The first testing task involved setting up a test bed capable of demonstrating an S-band limiter. S-band simply refers to a range of frequencies within the microwave region of the electromagnetic spectrum. The range for S-band is 2 – 4 GHz, where as for X-band it is 8 – 12 GHz. A schematic of the test bed is shown in Figure 3. The voltage and current from the high power supply of our X-band radar system were measured to determine that they were compatible with and able to drive the S-band magnetron. A magnetron is simply a microwave generator, similar to the source in a microwave oven. After confirmation, the leads to the X-band magnetron were disconnected, brought outside the cabinet, and connected to the S-band magnetron. Upon pulsing the magnetron, an RF output pulse of the expected power level and duration was measured.

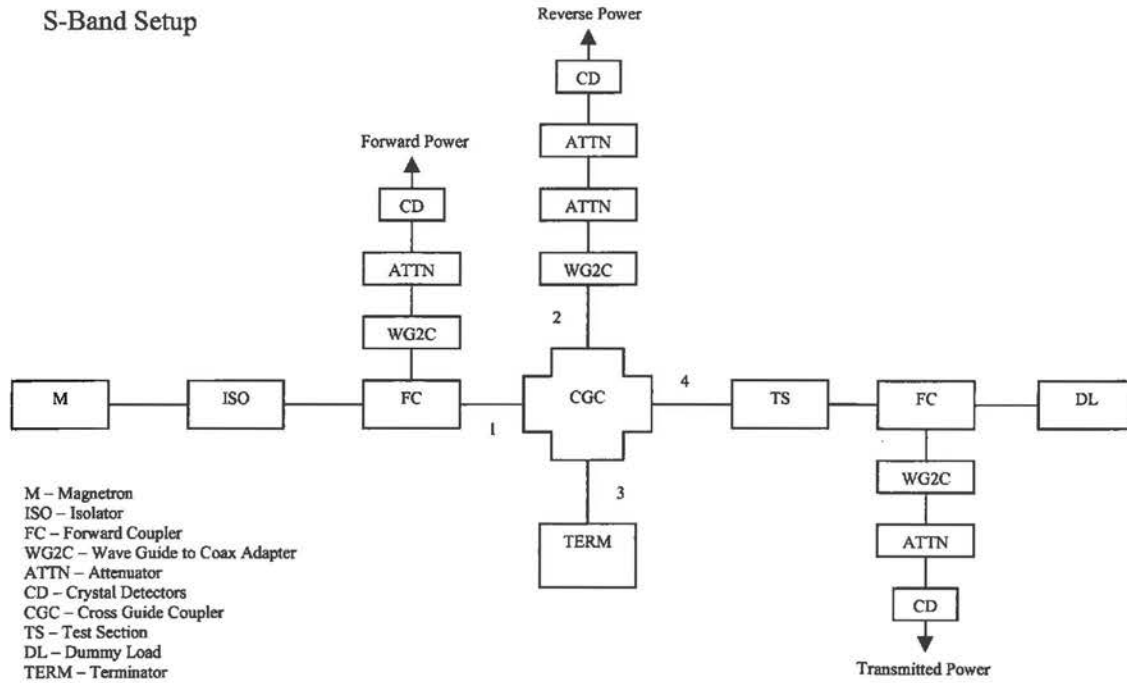


Figure 3: S-band Setup

The S-band test bed assembly is shown in Figure 4. The magnetron (Figure 5) is driven by the primary power circuit in the X-band radar system. The magnetron is pulsed through an external sync with a high-voltage trigger source.



Figure 4: S-band Test Bed Assembly



Figure 5: S-band Magnetron

The S-band plasma limiter test section is on the right side of Figure 4. It was designed to utilize a 12" section of S-Band rectangular waveguide with end flanges. The waveguide section as manufactured was not vacuum tight, so the flanges were rebrazed.



Figure 6: Test Section

A close up of the test section is shown in Figure 6. It has been fully installed into the test bed with vacuum system and the needle positioning apparatus attached. After the test bed was assembled, a 8720C Hewlett Packard Network analyzer was used to measure the insertion loss and isolation of the waveguide parts. Insertion loss refers to the attenuation of the overall signal due to the insertion of given part into the assembly. The higher the insertion loss, the more the signal is attenuated causing less signal power to propagate and be received by downstream electronics.

A basic test matrix to verify the operation of the plasma limiter in an S-band waveguide configuration was performed. A halogen gas mixture was used as the breakdown medium. Breakdown data was recorded across a pressure range to determine the breakdown activation level dependence on pressure. In addition, gap distance (needle depth) was varied, and active biasing was used to determine the impact of pre-ionization on limiter performance.



Figure 7: Limiter Breakdown Data: The yellow curve represents input power. The green curve, or transmitted power, increases with the incident power until a threshold level is reached. At that time the plasma is fully operational, begins to reflect all incident power, and causes transmitted power to go to zero.

Figure 7 shows data from a plasma limiter in operation. Note that the transmitted curve begins to rise with the incident pulse, however, once the threshold value for breakdown is reached the plasma limiter device activates reflecting all of the incident power. The transmitted channel drops to zero, and the reflected channel follows the incident pulse. The reason the reflected power does not equal the incident power, even though the transmitted power is zero, is due to the attenuation of the various transmission components coupled with the absorption properties of the forming plasma.

An initial experiment was performed to generate a Paschen curve of breakdown strengths versus gas pressure as shown in Figure 8. Five limiter activations were generated at seven different pressures. The peak activation power for each shot is shown in Figure 8. As can be seen, there exists a clear minimum in the breakdown power levels. This data is in agreement with the predicted results. Also, at each pressure the statistical nature of the breakdown phenomenon is apparent.

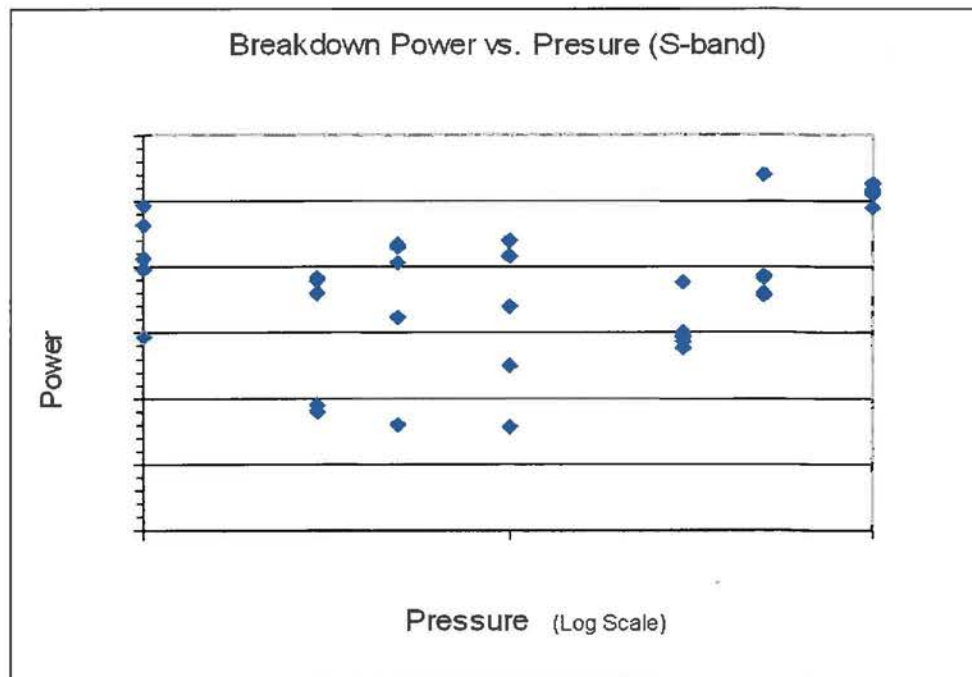


Figure 8: Paschen Curve for Halogen Gas Mixture

Once we had an optimal pressure the effect of needle insertion depth on limiter performance was explored. At this pressure, limiter breakdown levels were measured for needle insertion depths of 25, 50, and 75 percent of the total waveguide height (Figure 9). No direct

dependence on needle depth is evident. All three needle positions show roughly the same minimum breakdown level within the statistical spread. It was also concluded that insertion loss due to the depth of the needle was insignificant to the overall system operation.

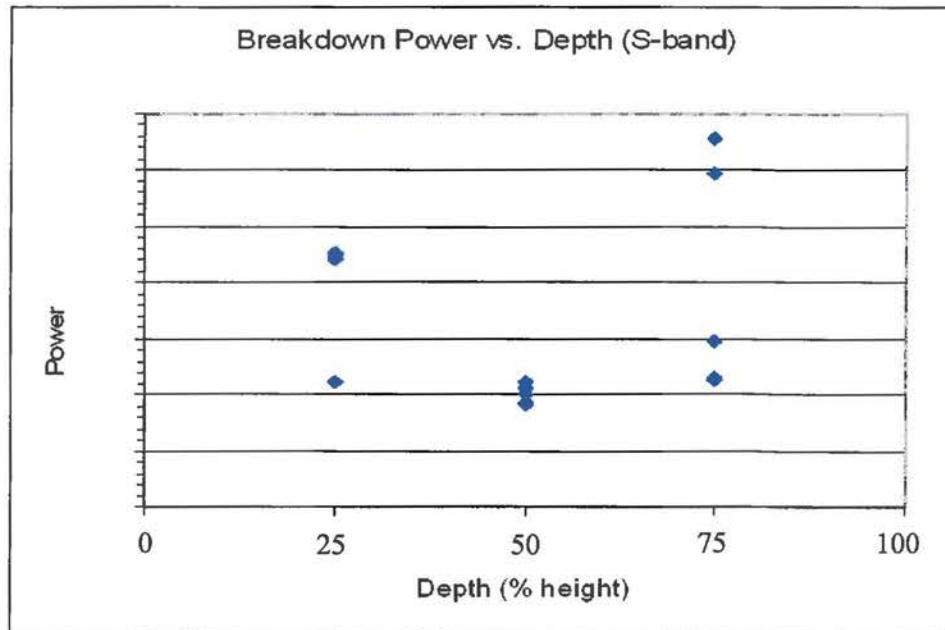


Figure 9: Needle Insertion Depth

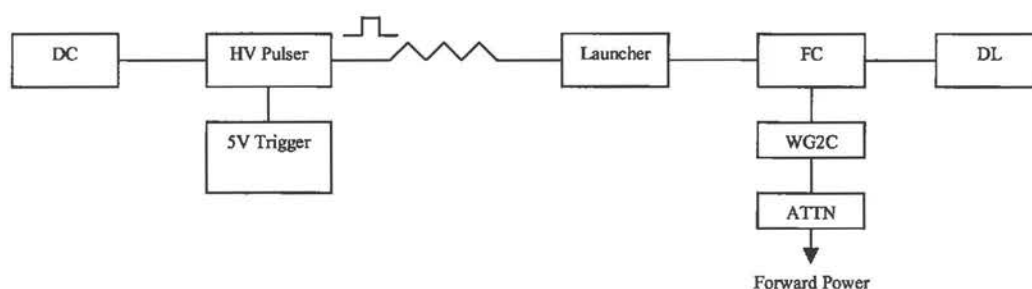
Once these optimal settings were determined, the magnetron was turned on allowing microwaves to propagate down the waveguide. When the incident power of these microwaves exceeded the threshold power, the limiter was activated. When the plasma limiter activates, a plasma region is formed around the tip of the needle. This plasma is conductive and hence reflective to the incoming RF power. The physical extent of the plasma is directly related to the ability of the plasma to fully attenuate all incoming microwaves. The plasma encompassed the tip of the needle and the surrounding region. Thus an S-band plasma limiter was shown to activate at a minimum incident power level and provide adequate attenuation for electronic protection.

Development of UWB Source

In addition to protection against single frequencies located in the S-band range, the plasma limiter must be able to function against bursts of multiple hostile frequencies at a time. To test this functionality, a HPM pulse generator was constructed. Figure 10 shows the setup for

the UWB pulse generator. The pulse generator utilizes the waveguide launcher from the S-band magnetron, modified into a spark gap configuration. A capacitor discharging through a resistor allows a fast rise time pulse propagating through the waveguide. A waveguide flange was modified with a pressure feed through. This flange fed a halogen gas mixture into the spark gap to increase the voltage hold off and decrease pulse rise time.

UWB Setup



DC – DC Power Supply
 HV Pulser – High Voltage Pulser
 FC – Forward Coupler
 DL – Dummy Load
 WG2C – Wave Guide to Coax Adapter
 ATTN – Attenuator

Figure 10: UWB Setup

Figure 11 shows the modified launcher from the S-band magnetron. Inside the launcher is the modified spark gap setup including the dielectric cylinder and corresponding anodes. The anodes are held within the dielectric by a bolt which is used to vary the spark gap distance between the anode and the launcher. The cylinder is then placed inside the launcher creating this gap and a high voltage is connected to the resistor which is then connected with the bolt.



Figure 11: UWB Launcher Setup

After successful testing on the UWB was done, response/power level measurements were made. Maximum observed output and pulse rise time met our requirements and predicted values. Some early data was collected using an Agilent 54855A oscilloscope and processed using Matlab. In our “Frequency content of pulse” plot, it was found that the main frequency component is centered on ~ 3 GHz having ~ 1.5 GHz bandwidth. It was also found that minor components were obtained at ~ 6 GHz and ~ 500 MHz. It has been determined that the 500 MHz component is due to noise pickup at the scope from radiation of power at the high voltage resistor (500 MHz will not propagate in any S-Band waveguide) [10]. From this data it was determined that a UWB generator with an acceptable frequency spread had been constructed and that UWB testing could proceed.

The problem of noise radiation has since been corrected by obtaining smaller physical size resistors and shielding them with a metal radiation enclosure attached to the launcher. This shield housing was constructed to prevent the noise signal from escaping into the surrounding environment. The wideband generator and shield housing are shown in Figure 12.



Figure 12: Wideband generator and metal EMI housing

Initial testing of our limiter against this device shows semi-adequate suppression of UWB. However, optimizations will be made and more data will be taken from this device later.

Development of TE_{20} Limiting

In performing the initial and UWB testing it was determined that there was a possibility of higher order modes beyond TE_{10} propagating down the waveguide. The limiter must also be able to protect against these modes, so a new section for parametric testing of multiple needle configurations was designed and fabricated. To adequately test this multiple needle test section, a TE_{20} launcher was also designed and constructed.

Before a discussion of the development and testing of TE_{20} limiting, it is necessary to understand what TE waves are and why the analyses of various modes within TE waves are important. First, TE is a type of electromagnetic wave in which the component of the electric field in the direction of propagation is zero, hence the name transverse electric. There are other types of waves such as the TM (transverse magnetic) where this component of the magnetic field is zero and the TEM which is a combination of the two. The latter two types are not applicable to our experimentation. In general, radar and other similar systems only detect the TE_{10} mode propagating in the waveguide. The m and n in TE_{mn} are integer variables related to the harmonics which are possible to propagate in a given medium with a fixed width and height. What is important though is that the TE_{10} mode has its peak power located at the center of the waveguide, whereas other modes, specifically the TE_{20} , can have zero power being transmitted down the center of the waveguide. It then becomes clear that if a limiting device is built to only detect power in the TE_{10} mode, it is possible that harmful HPM which are propagating in higher frequencies and higher order modes could become transparent to this limiting device.

In order to evaluate the effects of these higher frequencies and higher order modes on our limiter's operation, we use an X-band magnetron to launch the TE₂₀ mode through the limiter. The magnetron sends a pulse into a wave splitter, which evenly divides the power into two signals that are opposite phase. These two signals are then launched side-by-side into a waveguide, creating the TE₂₀ mode. The resulting signal is transitioned from double wide X-band waveguide to S-band waveguide through a tapered section, and the final waveform is characterized in a subsequent measurement section before propagating through the limiter. Figure 13 gives a schematic of the setup [11].

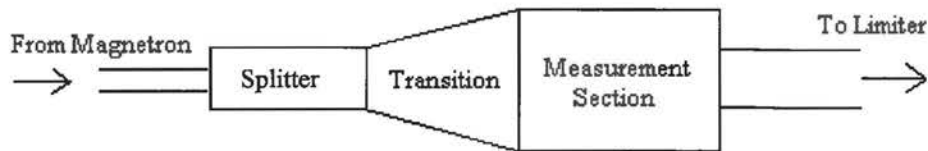


Figure 13: TE₂₀ Schematic

Since most of the parts we needed to accomplish this task are not available for purchase, it was necessary that we design and build several items, including the transition section, a flange for the wave splitter, the measurement section, and the testing section. These pieces are put together to make the assembly shown in Figure 14.

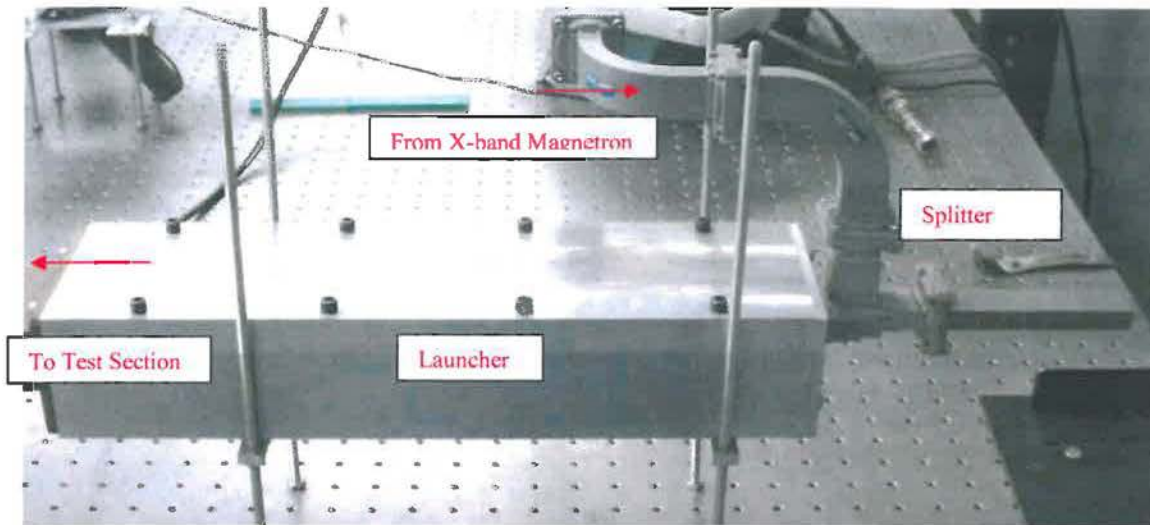


Figure 14: TE₂₀ Launcher and Transition Section

The wave splitter was then connected to the transition section by means of a custom flange (Figure 15). The flange is tightly fitted to the tee and attached to it using a conductive epoxy, and bolts hold the flange tight to the transition assembly. The measurement section simply consists of a sliding probe attached to a straight section of waveguide, as illustrated in Figure 16. The probe is used to measure the power distribution transverse to the direction of propagation, thereby revealing the presence or absence of the TE₂₀ mode. In order to preserve the propagation characteristics of the waveguide, the slide was made from the same material as the waveguide and flush with its interior.

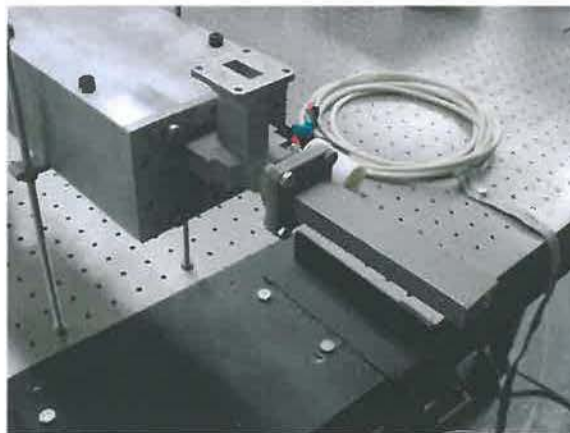


Figure 15: Wave Splitter & Flange

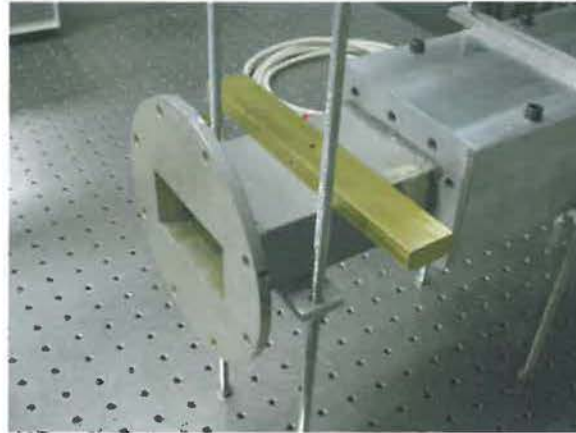


Figure 16: Sliding Probe

To test the higher order mode propagation within the waveguide, a multiple needle test section was designed. Specifically we tested the limiters ability to protect against damaging pulses that propagate in the TE_{20} mode. Figure 17(a) shows the theoretical power distribution of this mode versus the normalized width of the wave guide. The figures show a cross-section of the waveguide transverse to the direction of propagation. It should be noted that, in contrast to the dominant TE_{10} mode where the power density is maximum at the center of the waveguide, the power density maximums in the TE_{20} mode are located at the quarter widths of the guide. The null at the center will allow power contained in higher order modes, namely TE_{20} in this case, to pass the single needle protection device uninhibited. Figure 17(b) shows the wave profile of the constructed TE_{20} launcher. Again, the points to note are the peaks of the wave profile shown are at 25 and 75 percent widths of the guide and the null located at the center [11]. The measurements were taken with a movable slider probe that was constructed from a piece of waveguide previously shown in Figure 16.

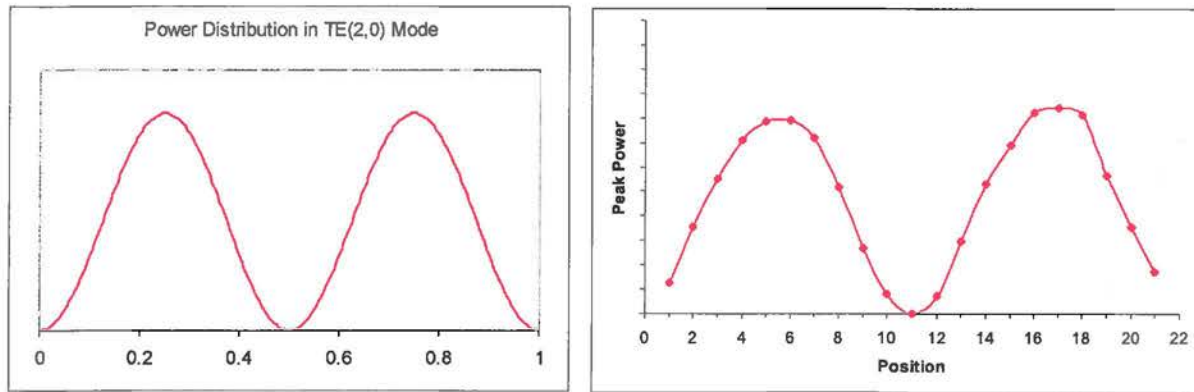


Figure 17: (a) Calculated power distribution in TE_{20} mode (b) Measured values of constructed TE_{20} launcher

Figure 18 shows the setup for the TE_{20} test. A pulsed magnetron is directed into the launcher section which is located prior to the needle test section, slider probe used for measurement, and a dummy load.

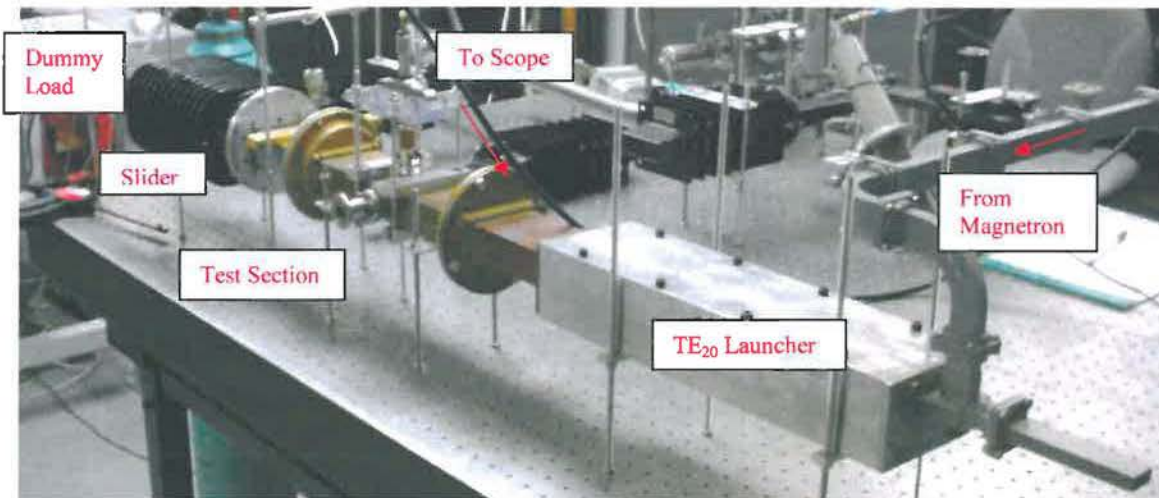


Figure 18: TE_{20} Test Arrangement

As anticipated, preliminary tests conclude that the single needle configuration of the test section did not cause plasma breakdown when exposed to the TE_{20} mode. In order for a receiver protector to prevent propagation of power past the device, a multiple needle configuration is required.

To test the limiter versus this higher order mode (which conventional receiver protectors ignore) we have designed a multiple needle limiter test section that can accommodate this shift in the power density maximums. Figure 19 shows the multiple needle test section.



Figure 19: Multiple Needle Test Section

Figure 19 shows the waveguide section (1), the vacuum plate (2), the rotating needle section (3), and the needle inserts (4) of the multiple needle test section. In the horizontal position, the rotating needle section has needle locations placed at 0.25, 0.5, and 0.75 of the normalized width of the guide. Since the section is rotatable, this test apparatus can also accommodate even higher order modes, such as the TE_{30} mode, and can produce multiple needle configurations for testing against any of these modes.

These multiple needle configurations have the potential to improve limiter operations by lowering the threshold breakdown level (spike leakage), reducing the flat leakage, and/or decreasing the activation time [12]. The completed test section has a rotating table that is capable of placing 3 needles in a variety of configurations. The needle, holder, and rotating table are shown in Figure 20. The needle holder is constructed of specific materials to facilitate biasing of the needle.



Figure 20: Needles and Rotating Needle Holder Plate

Initial testing on the TE_{20} mode was performed upon completion of the multiple needle test section. Output wave characterization is shown below in Figure 21. Results showed that although the plasma breakdown occurred within the limiter in TE_{20} mode it has a less than optimal rise time, often allowing a spike of the (almost) peak power to propagate through the limiter. An increase in the frequency pulse rate was often required to initiate plasma breakdown. Once breakdown had occurred, the pulse rate could then be backed off and breakdown would continue.

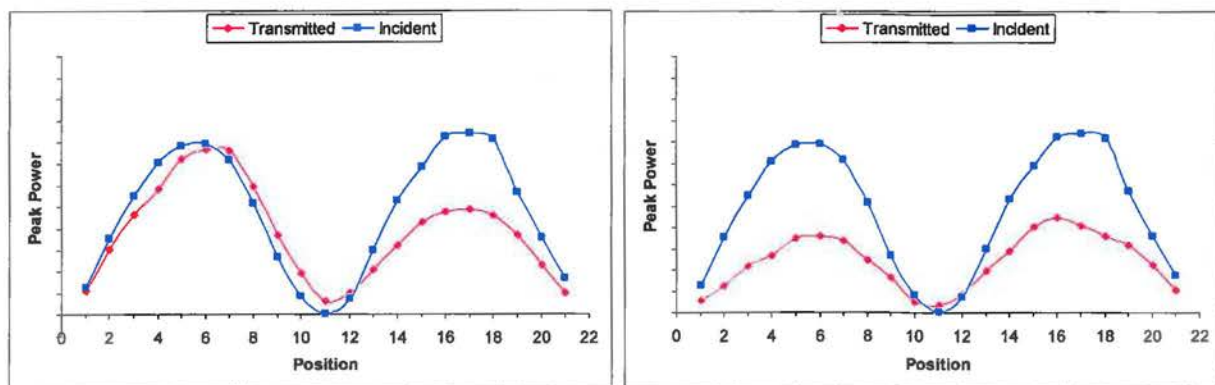


Figure 21: Limiter Transmission with Two Needles (a) and Three Needles (b)

It was concluded that the multiple needle limiter would work in a TE_{20} or higher mode environment. However, optimizations to limit the peak power propagation to an acceptable level would need to be performed. It is worth noting that average power was limited very well.

Conclusions

This experimental work was conducted in an S-band test bed to simulate a pulse from a fixed frequency high power RF source. Successful repetitive limiting breakdown phenomena were observed in a halogen gas mixture at various pressures for the TE₁₀ mode. It was found that the plasma limiter worked very well and efficiently as a protection device against HPM in this normal mode.

In the process of testing, several failure modes were discovered and experimentation was undertaken to test how the limiter would respond to these areas of possible failure. First, UWB testing was performed. Having already successfully tested the limiter's ability to protect against single frequencies located in the S-band range, the UWB experiments further tested the plasma limiter's ability to function against bursts of multiple hostile frequencies at a time. Results from these test varied with the optimizations. Final testing in the UWB failure mode showed successful plasma breakdown, but propagation of a higher than optimal power leakage spike.

It was also determined that there was a possibility of higher order modes beyond TE₁₀ propagating down the waveguide. The limiter must also be able to protect against these modes, so a new test section allowing multiple needle configurations and a TE₂₀ mode launcher were designed and constructed. Testing showed that the multiple needle limiter would work in a TE₂₀ or higher mode environment.

In both the UWB and the TE₂₀ testing, further optimization of the limiter should lead to lower breakdown levels and better overall performance. However, the goal of the project was met and a limiter which has extremely fast turn-on times, simple geometry, the ability to easily integrate into existing equipment, and requires no active pre-ionization equipment was constructed, designed, and proven to work effectively as a protection device against HPM.

References

1. J. Wilson. *Popular Mechanics*, “E-Bomb”, September 11, 2001.
2. L. Elliott, C. Murphy, and F. Vine. *Phase I Final Report*, AAC Internal Report, April 2004.
3. E. Nasser. *Fundamentals of Gaseous Ionization and Plasma Electronics*, Wiley Interscience, New York, 1961, p.140-141.
4. Y. Raizer. *Gas Discharge Physics*, Springer, Berlin, 1997, p.70-71 & 263-264.
5. Ibid, p.342-343.
6. J.S. Townsend. *Electricity in Gases*, Oxford University Press, 1915.
7. E. Nasser. *Fundamentals of Gaseous Ionization and Plasma Electronics*, Wiley Interscience, New York, 1961, p.141 & 246.
8. Ibid, p.254.
9. Ibid, p.304-334.
10. C. Murphy. *Phase II Monthly Report #3*, AAC Internal Report, September 2005.
11. C. Murphy. *Phase II Monthly Report #4*, AAC Internal Report, November 2005.
12. C. Murphy. *Phase II Monthly Report #5*, AAC Internal Report, January 2006.

graduates in May

**Southern Scholars Honors Program
Senior Project**

Name Matthew Andersen

Date 2/8/06



Major CS, Math, Physics

Southern Scholars
southernscholars.southern.edu
wmclarty@southern.edu

A significant scholarly project, involving research, writing, or special performance, appropriate to the major in question, is ordinarily completed the senior year. The project is expected to be of sufficiently high quality to warrant a grade of A and to justify public presentation.

Under the guidance of a faculty advisor, the Senior Project should be an original work, should use primary sources when applicable, should have a table of contents and works cited page, should give convincing evidence to support a strong thesis, and should use the methods and writing style appropriate to the discipline.

The completed project, to be turned in in duplicate, must be approved by the Honors Committee in consultation with the student's supervising professor three weeks prior to graduation. Please include the advisor's name on the title page. The 23 hours of credit for this project is done as directed study or in a research class.

Keeping in mind the above Senior Project description, please describe in as much detail as you can the project you will undertake. You may attach a separate sheet if you wish:

See Attached

Signature of faculty advisor Chris Han Expected date of completion 21 April, 2006

This project has been completed as planned (date) 14 April, 2006

This is an "A" project A This project is worth 2-3 hours of credit 2

Advisor's Final Signature Chris Han

Chair, Honors Committee _____ Date Approved _____

Dear Advisor, please write your final evaluation of the project on the reverse side of this page. Comment on the characteristics that make this A "quality work."

Matt Andersen
Senior Project Summary – Southern Scholars

Very Quick Description: To develop and test a working S-band plasma limiter.

Directed Energy (DE) from High Powered Microwaves (HPM) and Ultra Wide Band (UWB) radio frequency (RF) sources, pose a serious threat to today's electronic systems. This electronic equipment, whether consumer, business, or government, is susceptible to many things ranging from lightning or home power surges to EMP bombs. Plasma limiters can provide highly reliable, front-end protection from this threat in a low-cost, easily implemented manner.

Simply described, plasma limiters are "fuses" that protect sensitive electronics from disruption or destruction by high power RF. Limiters are normally passive and do not affect the operation of the circuitry. However, when a high power RF pulse is incident, the limiter is activated. As long as the threat energy is present, the transmitted power is 'limited' to a threshold level and the damaging energy of the incident power is reflected. Once the RF pulse ceases, the plasma limiter recovers and returns to its normally passive state.

Currently, two types of transient suppression devices capable of providing high RF power protection exist. The first is solid state devices such as metal oxide varistors (MOV) and silicon avalanche diodes. These devices have fast activation times, but are limited in the incident power they can withstand. The second type is conventional gas-discharge tubes. These tubes are essentially spark gaps in which an arc discharge occurs when a RF pulse is applied. They can withstand more power than the solid state devices but have a slower activation time.

The initial goal of this project, which was completed about six months ago, was to prove the feasibility of a plasma limiter in a S-band waveguide configuration capable of 1) sub-nanosecond response time, and 2) the ability to reflect high peak and average incident disruptive RF power. The challenge in developing such a device lies in the fact that these two performance characteristics are always incompatible with conventional transient protective devices. For example, solid state devices such as silicon avalanche diodes have extremely fast turn-on times (< 1 psec) and even high peak power capability (> 100 kW) but have low average power handling capability (< 10 W). Conversely, conventional gas discharge tubes can easily handle average powers > 10 kW but have inherently slow turn-on times (> 100 nsec).

The current goal of this project is to develop a working proof of principle demonstration of an S-band plasma limiter which displays the best characteristics of both: large power handling capability and fast response time. The technical challenges are:

- UWB source design and development,
- Mixed / multimode testing,
- Test section design and fabrication,
- Ultra fine needle positioning, and
- Easily integrated into existing equipment.